

Hafnium intercalation between epitaxial graphene and Ir(111) substrate

Linfei Li, Yeliang Wang, Lei Meng, Rong-ting Wu, and H.-J. Gao

Citation: *Appl. Phys. Lett.* **102**, 093106 (2013); doi: 10.1063/1.4793427

View online: <http://dx.doi.org/10.1063/1.4793427>

View Table of Contents: <http://apl.aip.org/resource/1/APPLAB/v102/i9>

Published by the [American Institute of Physics](#).

Additional information on *Appl. Phys. Lett.*


Journal Homepage: <http://apl.aip.org/>

Journal Information: http://apl.aip.org/about/about_the_journal

Top downloads: http://apl.aip.org/features/most_downloaded

Information for Authors: <http://apl.aip.org/authors>

ADVERTISEMENT



AIP | Applied Physics Letters

Accepting Submissions in
Biophysics and Bio-Inspired Systems

Submit Today

AIP
Publishing

Hafnium intercalation between epitaxial graphene and Ir(111) substrate

Linfei Li, Yeliang Wang,^{a)} Lei Meng, Rong-ting Wu, and H.-J. Gao^{a)}

Institute of Physics, Chinese Academy of Sciences, Beijing 100190, China

(Received 3 December 2012; accepted 11 February 2013; published online 5 March 2013)

We report on the change of structural and electronic properties while depositing Hf atoms onto the graphene epitaxially grown on Ir(111) substrate. We find that the Hf atoms intercalate between the graphene and its iridium host. This intercalation induces a new interface superstructure, as confirmed by scanning tunneling microscopy and low energy electron diffraction. Raman spectra reveal that the Hf-intercalated graphene shows the prominent features of intrinsic graphene. Our study suggests that the Hf intercalation acts as a buffer layer between the graphene and the Ir(111) substrate, restoring the graphene's intrinsic electronic properties. © 2013 American Institute of Physics. [<http://dx.doi.org/10.1063/1.4793427>]

High quality graphene (G), owing to its unique band structure, ultrahigh carrier mobility, and many corresponding potential applications,^{1–3} is considered to be one of the most promising materials for future electronics. Among the several major growth methods of graphene, epitaxial growth on transition metal substrates, which act as both template and catalyst, has proven to be an effective route to fabricate high quality and large-scale graphene.^{4–7} However, strong interaction generally exists at the interface of the graphene and the metal substrate, disrupting the characteristic linear π -bands of graphene near the Fermi level and, therefore, strongly suppressing the intrinsic electronic properties of graphene. For example, high quality graphene can be fabricated on Ir(111) crystal,^{8,9} but its π band is hybridized with the Ir 5d state. This hybridization affects the intrinsic electronic structure of graphene to some degree, causing invisibility of the vibrational states of graphene prepared on Ir(111) surface in Raman spectra.¹⁰

An attractive approach to screen this interaction and decouple the epitaxial graphene from the metal substrate is to introduce a buffer layer at the interface of the graphene and its metal host, such as intercalated metal atoms,^{11–14} small molecules,^{15,16} or even semiconductor silicon atoms.^{17,18} For instance, Au, Pt, Ni, and alkali metals^{11–14} have been intercalated as buffer layers into graphene/metal interfaces, and they indeed tune the coupling of graphene with the metal substrate. In the present study, we focus on Hf intercalation under graphene on Ir(111). Our experiments presented here were motivated by the intercalation of silicon^{17,18} and oxygen,^{15,16} and the eventual formation of a SiO₂ layer between the graphene and the metal (G/SiO₂/metal), reported recently.¹⁹ The insulating SiO₂ interface layer formed underneath the graphene makes it feasible to measure and explore the transport properties of epitaxial graphene prepared on metal substrates. As a matter of course, the similar and preferred G/HfO₂/metal heterostructure is desired owing to its better performance in microelectronic devices (higher dielectric constant of HfO₂ compared with SiO₂).²⁰ As the first and crucial step, hafnium intercalation between graphene and metal substrate will be

studied here, including the topographic and electronic properties at the interface.

The growth of high quality graphene was performed by the thermal decomposition of ethylene (C₂H₄), which was catalyzed by a heated Ir(111) substrate. And then hafnium was deposited on the G/Ir(111) sample, and the sample was subsequently annealed. Low energy electron diffraction (LEED) and scanning tunneling microscopy (STM) were employed to characterize the differentiated superstructures and topographies of the sample before and after annealing treatment. We consider that the new superstructure emerging after annealing results from the hafnium intercalation. Moreover, we studied the electronic properties of the system by means of Raman spectroscopy on both G/Ir(111) and G/Hf/Ir(111) samples, further confirming that the hafnium intercalation does indeed decouple the interaction of graphene with the Ir substrate.

More specifically, experiments were carried out in an ultrahigh vacuum system with a base pressure in the 2×10^{-10} mbar range equipped with a variable temperature STM, an Ar⁺ sputtering gun, a LEED device, a hafnium electron beam evaporator, a gas doser for ethylene, and so on. A clean Ir(111) substrate was prepared by repeated cycles of Ar⁺ sputtering and annealing at 1470 K. Graphene was fabricated via exposure of the Ir(111) surface to ethylene atmosphere for 80 s at a certain temperature followed by an annealing step at 1570 K. The hafnium was deposited on the G/Ir(111) at room temperature from the E-beam evaporator, in which the hafnium flux can be controlled at a constant value. Hafnium intercalation under graphene occurred when the sample was annealed at 673 K. Raman spectra were obtained by a Renishaw spectrometer at 532 nm with 1 mW power.

The as-prepared graphene on Ir(111) surface was first characterized by STM imaging. Figure 1(a) shows a typical STM topography of graphene, where we can see a well ordered moiré superstructure with 2.52 nm periodicity. Such a moiré pattern results from the mismatch between the graphene unit cell and the Ir(111) lattice. The inset of Fig. 1(a) represents the atomically resolved STM topography of the graphene adlayer, in which the direction of honeycomb structure is in parallel with the close-packed [1 $\bar{1}$ 0] direction of the Ir(111) substrate.

^{a)}Electronic addresses: ylwang@iphy.ac.cn and hjgao@iphy.ac.cn.

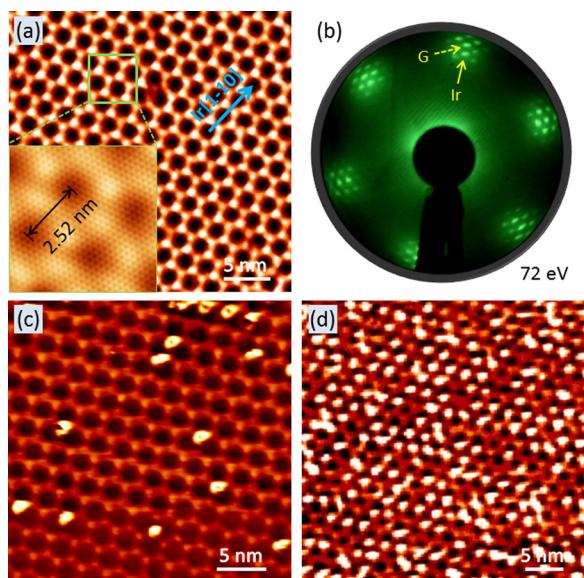


FIG. 1. STM topographic images and LEED pattern of graphene on Ir(111) surface before and after hafnium deposition. (a) STM image ($U = -0.67$ V, $I = 0.07$ nA) from a graphene layer grown on Ir(111), showing a moiré superstructure with a periodicity of 2.52 nm. The inset (5 nm \times 5 nm) is a zoomed-in image with atomically resolved honeycomb lattice of graphene adlayer. (b) The corresponding LEED pattern from G/Ir(111) sample shown in (a). The spots resulting from the Ir(111) lattice and graphene lattice are indicated by solid-line arrow and dashed-line arrow, respectively. (c) STM image (-2.30 V, 0.03 nA) obtained at the sample after Hf deposition on G/Ir(111) at room temperature. (d) STM topography (1.0 V, 0.02 nA) of Hf-deposited G/Ir(111) surface after increasing Hf coverage.

Furthermore, the macroscopic quality of graphene was examined by LEED. As shown in Fig. 1(b), the symmetric LEED pattern consists of six pairs of spots. The inner spot and outer spot of each pair, indicated by the solid-line and dashed-line arrows, originate from the Ir(111) lattice and graphene adlayer, respectively. The additional satellite spots surrounding the Ir spots in a hexagonal pattern signify the moiré superstructure of graphene, which is clearly visible in Fig. 1(a). Besides, the fact that the directions of the G spots and Ir spots coincide indicates that the orientation of the graphene lattice is parallel to the Ir substrate, which is consistent with the STM topography in Fig. 1(a). Therefore, on the basis of the STM images and the LEED pattern, we can conclude that large area graphene with a consistent orientation has been prepared on Ir(111) surface.

Then, deposition of Hf onto the resulting graphene/Ir(111) surface was carried out at room temperature. Figure 1(c) illustrates the G/Ir(111) surface covered with a few Hf clusters, which prefer to occupy the fcc and hcp sites of graphene moiré pattern, the former especially. Subsequently, when we increased the Hf coverage, the clusters occupied more fcc sites and resulted in a regular distribution on the graphene adlayer, as displayed in Fig. 1(d). Additionally, LEED was performed on the as-deposited surface and no significant change was found compared with the pattern in Fig. 1(b) except for the more diffusing background resulting from the deposited Hf clusters (not shown here), suggesting that the clusters were still above rather than beneath graphene adlayer (in the latter case, the element intercalation would generally disrupt the moiré feature¹⁶ and the corresponding satellite spots^{21–23}), which is consistent with the STM topographies in Figs. 1(c) and 1(d).

After we annealed the as-deposited sample at 673 K, the topmost Hf clusters disappeared and new superstructure emerged on the sample, as revealed by the STM image in Fig. 2(a). Such a well-ordered superstructure has a periodicity of 0.54 nm, twice the periodicity of the Ir(111) unit cell. In addition, the original 2.52 nm moiré pattern of graphene become fuzzy. We speculated that the new 0.54 nm superstructure results from the intercalated hafnium and that it is the hafnium intercalation that weakens the graphene-Ir interaction and leads to the fuzzy moiré pattern as a result. In order to further support the assumption, LEED was employed to record the same sample surface. As can be seen in the LEED pattern in Fig. 2(b), additional (2×2) diffraction spots indicated by the dotted-line arrow are clearly visible, which correspond to the new superstructure observed in Fig. 2(a). In addition, it is noteworthy that the satellite spots are faint and barely visible in comparison to the unannealed sample, which is in agreement with the fuzzy 2.52 nm moiré pattern in Fig. 2(a).

In order to probe the graphene lattice which was considered to be the topmost overlayer of this heterostructure system, we let the scanning tip gradually approach the sample surface by varying scanning parameters. And then, we obtained the STM image in Fig. 2(c) recorded from the same scanning region as in Fig. 2(a). In the lower part of this image, the same (2×2) superstructure as that in Fig. 2(a) is observed. The corresponding profile along the blue-line

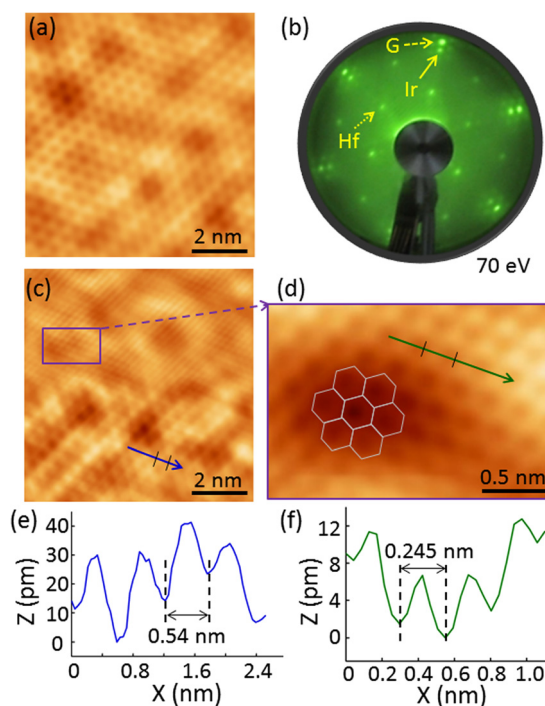


FIG. 2. STM images and LEED pattern of graphene on Ir(111) after Hf intercalation. (a) STM topography ($U = -0.80$ V, $I = 0.50$ nA) of Hf-intercalated graphene on Ir(111) with fuzzy moiré pattern. A (2×2) superstructure with respect to Ir(111) lattice is clearly visible. (b) The corresponding LEED pattern from the G/Hf/Ir sample in (a). One Hf diffraction spot is indicated by the dotted-line arrow. (c) STM image recorded from the same surface region as (a) shows the (2×2) superstructure and graphene lattice (the lower image part: -0.77 V, 0.55 nA; the upper part: -0.75 V, 0.87 nA). (d) A zoomed-in image in the surface region indicated by the purple rectangle in (c). Graphene's honeycomb lattice, indicated in gray, is visible. (e) and (f) Profiles along the blue and green lines in (c) and (d), respectively.

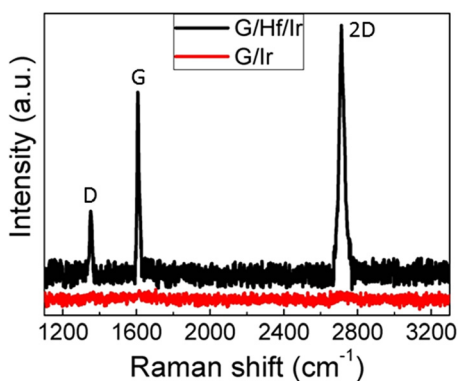


FIG. 3. Raman spectra from graphene grown on Ir(111) surface before and after Hf intercalation. The characteristic Raman features of graphene, G peak and 2D peak, are visible in the Hf-intercalated sample but invisible in the pre-intercalation sample.

arrow in this part is shown in Fig. 2(e). In this profile, the distance of 0.54 nm between two adjacent valleys further confirms the identical (2×2) superstructure. Apart from this superstructure, we can find another structure with a smaller periodicity, as revealed in the upper part of Fig. 2(c). Correspondingly, a zoomed-in STM image of this part is displayed in Fig. 2(d). We can see the intact characteristic honeycomb structure of graphene, which is consistent with the clear G spots in reciprocal space [LEED pattern in Fig. 2(b)]. Furthermore, the profile of this image shows a periodicity of 0.245 nm [see Fig. 2(f)], providing a direct proof of graphene lattice.⁸

From the foregoing, we can come to a brief summary that hafnium intercalation underneath graphene on Ir(111) surface has been accomplished and the resulting superstructures are demonstrated by STM and LEED. Further, in order to characterize the physical properties of the Hf-intercalated graphene from the macroscopic perspective and examine the effect of Hf intercalation on the coupling of graphene with the metal substrate, Raman spectroscopy was performed both on the Hf-intercalated graphene and the pristine graphene on Ir(111) surface. As we can see in Fig. 3, no Raman signal of graphene is found on the G/Ir sample before Hf intercalation, indicated by the red line, which is ascribed to the mixing of the π bands of graphene and the Ir 5d state.¹⁰ After Hf intercalation, by contrast, the characteristic Raman spectrum of graphene, including the G peak and the 2D peak, emerged from the G/Hf/Ir surface. The reasonable explanation is that the intercalated Hf atoms at the G/Ir interface decouple the graphene from the metal substrate and restore the intrinsic electronic properties of graphene. In addition, we notice the presence of the D peak in the Raman curve comparing to that of G/Si/Ir system.¹⁷ The coverage of graphene in present system is less than 1 ML and there are isolated graphene domains on the substrate. The edges of these domains would be mainly responsible to the D peak in the Raman spectroscopy.^{24–26}

In conclusion, by using STM, LEED, and Raman spectroscopy, we have studied the structural and electronic properties of the Hf-intercalated G/Ir(111) system. The deposited Hf atoms intercalated into the G/Ir interface when the sample

was annealed. The Hf intercalation as a buffer layer lifts the graphene overlayer from the metal substrate and enables effectively decoupling of the graphene-substrate interaction, therefore, recovering the graphene's intrinsic electronic properties. Our current study, as the first step of importance, makes it possible to fabricate a graphene/HfO₂/metal heterostructure by further intercalation of oxygen underneath graphene, which is expected to have wide application in microelectronics-oriented devices based on high quality graphene.

We would like to gratefully acknowledge financial support from MOST (Nos. 2011CB932700, 2010CB923004, and 2009CB929103), NSFC (No. 61222112), and CAS in China.

- ¹K. S. Novoselov, A. K. Geim, S. V. Morozov, D. Jiang, Y. Zhang, S. V. Dubonos, I. V. Grigorieva, and A. A. Firsov, *Science* **306**, 666 (2004).
- ²A. K. Geim and K. S. Novoselov, *Nature Mater.* **6**, 183 (2007).
- ³A. H. Castro Neto, F. Guinea, N. M. R. Peres, K. S. Novoselov, and A. K. Geim, *Rev. Mod. Phys.* **81**, 109 (2009).
- ⁴Y. Pan, D.-X. Shi, and H.-J. Gao, *Chin. Phys.* **16**, 3151 (2007).
- ⁵Y. Pan, H. G. Zhang, D. X. Shi, J. T. Sun, S. X. Du, F. Liu, and H.-J. Gao, *Adv. Mater.* **21**, 2777 (2009).
- ⁶K. S. Kim, Y. Zhao, H. Jang, S. Y. Lee, J. M. Kim, K. S. Kim, J. H. Ahn, P. Kim, J. Y. Choi, and B. H. Hong, *Nature* **457**, 706 (2009).
- ⁷L. Gao, J. R. Guest, and N. P. Guisinger, *Nano Lett.* **10**, 3512 (2010).
- ⁸A. T. N'Diaye, J. Coraux, T. N. Plasa, C. Busse, and T. Michely, *New J. Phys.* **10**, 043033 (2008).
- ⁹L. Meng, R. T. Wu, L. Z. Zhang, L. F. Li, S. X. Du, Y. L. Wang, and H. J. Gao, *J. Phys.: Condens. Matter* **24**, 314214 (2012).
- ¹⁰E. Starodub, A. Bostwick, L. Moreschini, S. Nie, F. E. Gabaly, K. F. McCarty, and E. Rotenberg, *Phys. Rev. B* **83**, 125428 (2011).
- ¹¹C. Enderlein, Y. S. Kim, A. Bostwick, E. Rotenberg, and K. Horn, *New J. Phys.* **12**, 033014 (2010).
- ¹²A. Varykhalov, J. Sanchez-Barriga, A. M. Shikin, C. Biswas, E. Vescovo, A. Rybkin, D. Marchenko, and O. Rader, *Phys. Rev. Lett.* **101**, 157601 (2008).
- ¹³L. Huang, Y. Pan, L. D. Pan, M. Gao, W. Y. Xu, Y. D. Que, H. T. Zhou, Y. L. Wang, S. X. Du, and H. J. Gao, *Appl. Phys. Lett.* **99**, 163107 (2011).
- ¹⁴A. Nagashima, N. Tejima, and C. Oshima, *Phys. Rev. B* **50**, 17487 (1994).
- ¹⁵P. Sutter, J. T. Sadowski, and E. A. Sutter, *J. Am. Chem. Soc.* **132**, 8175 (2010).
- ¹⁶H. Zhang, Q. Fu, Y. Cui, D. L. Tan, and X. H. Bao, *J. Phys. Chem. C* **113**, 8296 (2009).
- ¹⁷L. Meng, R. T. Wu, H. T. Zhou, G. Li, Y. Zhang, L. F. Li, Y. L. Wang, and H. J. Gao, *Appl. Phys. Lett.* **100**, 083101 (2012).
- ¹⁸J. H. Mao, L. Huang, Y. Pan, M. Gao, J. F. He, H. T. Zhou, H. M. Guo, Y. Tian, Q. Zou, L. Z. Zhang, H. G. Zhang, Y. L. Wang, S. X. Du, X. J. Zhou, A. H. C. Neto, and H. J. Gao, *Appl. Phys. Lett.* **100**, 093101 (2012).
- ¹⁹S. Lizzit, R. Larciprete, P. Lacovig, M. Dalmiglio, F. Orlando, A. Baraldi, L. Gammelgaard, L. Barreto, M. Bianchi, E. Perkins, and P. Hofmann, *Nano Lett.* **12**, 4503 (2012).
- ²⁰J. Robertson, *Rep. Prog. Phys.* **69**, 327 (2006).
- ²¹I. Gierz, T. Suzuki, R. T. Weitz, D. S. Lee, B. Krauss, C. Riedl, U. Starke, H. Höchst, J. H. Smet, C. R. Ast, and K. Kern, *Phys. Rev. B* **81**, 235408 (2010).
- ²²C. Virojanadara, S. Watcharinyanon, A. A. Zakharov, and L. I. Johansson, *Phys. Rev. B* **82**, 205402 (2010).
- ²³C. Riedl, C. Coletti, T. Iwasaki, A. A. Zakharov, and U. Starke, *Phys. Rev. Lett.* **103**, 246804 (2009).
- ²⁴A. C. Ferrari, J. C. Meyer, V. Scardaci, C. Casiraghi, M. Lazzeri, F. Mauri, S. Piscanec, D. Jiang, K. S. Novoselov, S. Roth, and A. K. Geim, *Phys. Rev. Lett.* **97**, 187401 (2006).
- ²⁵D. Graf, F. Molitor, K. Ensslin, C. Stampfer, A. Jungen, C. Hierold, and L. Wirtz, *Nano Lett.* **7**, 238 (2007).
- ²⁶L. M. Malard, M. A. Pimenta, G. Dresselhaus, and M. S. Dresselhaus, *Phys. Rep.* **473**, 51 (2009).